JOURNAL OF MATERIALS SCIENCE 31 (1996) 43–48

Fluxing of a 359/SiC/10p composite with alkali chlorides: effect of inclusions

F. H. SAMUEL, H. LIU
Département des Sciences Appliquées, Université du Québec à Chicoutimi, Chicoutimi (Québec), Canada, G7H 2B1

The effect of salt addition, in the form of a fluxing agent containing equivalent amounts of NaCl and KCl, on the microstructure and mechanical properties of 359/SiC/10p composite has been investigated. Both microstructure and properties are affected, with the removal of magnesium and strontium and the introduction of sodium and potassium being responsible for the degradation in properties. Thermodynamic calculations have been carried out to account for the effect of salt addition in terms of the surface adsorption of sodium and potassium impurities and the consequent changes in the surface–interface tension of their binary alloys. Mechanisms for the degradation of properties have been discussed.

1. Introduction

The normally observed inclusions in aluminum alloys are isolated fragments/films of aluminium oxide. The fragments are too thick and chunky to be newly formed oxide, but are almost certainly particles carried over from the melting furnace. These inclusions are extremely hard. During machining, they are often pulled out of the surface, causing defects on the machined surface. Film defects which affect the strength of castings are those caused in alloy mould systems where the surface film on the liquid metal is solid and where the film is caused to be entrained in the melt by surface turbulence [1].

Flux treatment has long been applied in the foundry of aluminium alloys to remove inclusions and to reduce the metallic content of skimmings and the dross generated. This treatment, however, cannot be applied to particulate reinforced metal matrix composites (MMCs), as the flux is known to remove the reinforcing particles from the melt. Schuster *et al.* [2] showed that when an MMC becomes too dirty to be recycled, the alumina or silicon carbide particles may be removed. This is accomplished by common salt or other fluxing techniques. It is thus possible to return the aluminium alloy matrix itself to the cleanliness level it was at, prior to having been processed into an MMC.

While the degradation effects of Na and K impurities on the mechanical properties of some aluminium alloys have been previously reported [3–5], so far not much information about their influence on MMCs is available in the literature, which led to this investigation.

1.1. Theoretical background

Defay *et al.* [6] have proposed a statistical thermodynamic model based for regular solutions. For this model, in the case of Al–Na alloy, for instance, the surface composition, X^S_{Na}, and the surface tension, γ^S, are given by

$$\frac{X^S_{Na}X^B_{Al}}{X^B_{Na}X^S_{Al}} = \exp(-\Delta H^S_a/RT) \quad (1)$$

and

$$\gamma^S = \gamma^S_{Al} + \frac{RT}{A}\ln\frac{X^S_{Al}}{X^S_{Na}} + l\frac{\omega_{Al\text{-}Na}}{A}[(X^S_{Na})^2 - (X^B_{Na})^2] - m\frac{\omega_{Al\text{-}Na}}{A}(X^B_{Na})^2 \quad (2)$$

where X^B_{Al} is the bulk concentration of Al; R, the gas constant; T, the melting point of the Al–Na alloy; ΔH_a, the heat of adsorption of Na on the surface; γ^S_{Al}, the surface tension of pure aluminium at melting; A, the specific surface area of the Al atoms; and $\omega_{Al\text{-}Na}$, the interaction parameter for Al–Na alloy.

Obviously, in the equations above, $X^S_{Al} = (1 - X^S_{Na})$ and $X^B_{Na} = (1 - X^B_{Al})$. For the face centred cubic structure in the case of aluminium, the value of l and m are 1/2 and 1/4, respectively. The heat of adsorption ΔH^S_a is calculated from the equation

$$\Delta H^S_a = A(\gamma^S_{Na} - \gamma^S_{Al}) + 2\omega_{Al\text{-}Na}(X^B_{Na} - X^S_{Na}) + 2\omega_{Al\text{-}Na}m(X^S_{Na} - 1/2) \quad (3)$$

where γ^S_{Na} is the surface tension of molten Na. The interaction parameter $\omega_{Al\text{-}Na}$ is defined as

$$\omega_{Al\text{-}Na} = Z[\varepsilon_{Al\text{-}Na} - (\varepsilon_{Al\text{-}Al} + \varepsilon_{Na\text{-}Na})/2] \quad (4)$$

where Z is the co-ordination number and equal to 12 in the case of aluminium. $\varepsilon_{Al\text{-}Na}$, $\varepsilon_{Al\text{-}Al}$ and $\varepsilon_{Na\text{-}Na}$ are the bond energies for Al–Na, Al–Al and Na–Na pairs, respectively.

0022–2461

TABLE I Chemical analysis of the matrix alloy composition of the NaCl contaminated specimens

Element	Si	Fe	Cu	Mg	Ti	Mn	Sr	Al
Specified concentration wt%	9.5–10.5	0.30 max	0.2 max	0.75–1.20	0.20 max	–	–	Remainder
Chemical analysis wt%	9.46	0.14	0.002	0.58	0.11	0.003	0.013	Remainder

2. Experimental procedure

The 359/SiC/10p composite used in the present work was received in the form of 12.5 kg ingots. The matrix alloy was modified with 140 p.p.m. Sr. Complete chemical analysis of the as-received charge is shown in Table I.

The ingots were cut into small pieces, preheated at 400 °C for 1–2 h prior to melting in a silicon carbide crucible of 7 kg capacity, heated with an electric resistance furnace (for more details see [6]).

Melts were contaminated with NaCl and KCl in two different ways

1. addition of pure NaCl powder, or,
2. addition of Foseco flux (45 wt % NaCl, 45 wt % KCl, 10 wt % $NaSO_4$) to the melt.

NaCl powder was introduced to the melt in concentrations of 10, 40 and 200 p.p.m. As the solubility of NaCl in molten aluminium is rather low and as NaCl has a lower density than aluminium, dissolution of NaCl in the composite was difficult to achieve. Various trials were made. Best dissolution was achieved when NaCl powder was wrapped in aluminium foil and placed in a hole drilled into a small block of the composite ingot, and the block then dipped into the melt.

Flux powders of ~ 1–2 wt % of the total charge were evenly scattered over the whole surface of the melt. Each addition of NaCl or flux powder was followed immediately by continuous mechanical stirring to promote the dissolution of NaCl or the flux powder in the melt. The melt was then cast into test bars using a permanent Stahl mould, at 20 min stirring intervals. Test bars were subjected to the T6 temper regime: solution treated for 8 h at 538 °C, followed by quenching in hot water at 60 °C, and by artificial ageing for 5 h at 155 °C. Tensile testing and microstructural examination were carried out using procedures mentioned elsewhere [7].

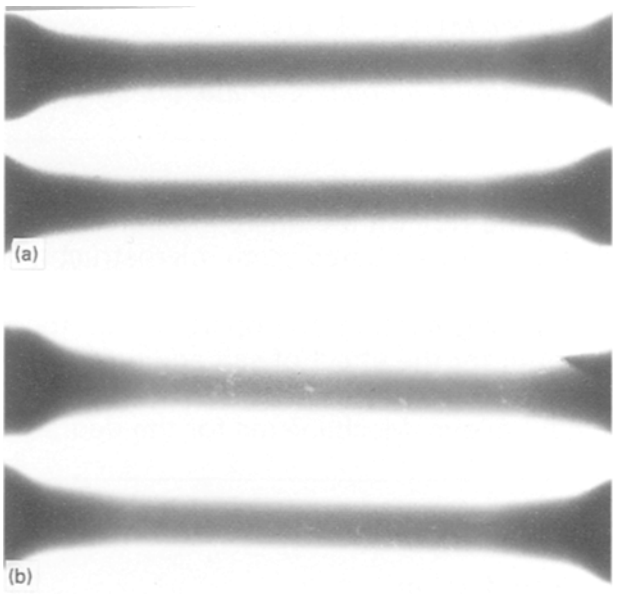

Figure 1 Radiographs obtained from (a) filtered, and (b) unfiltered composite test bars.

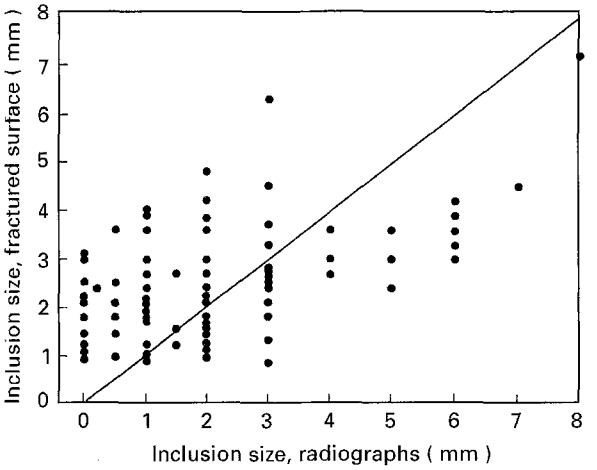

Figure 2 Inclusion size measured from radiographs versus inclusion size measured from fractured surfaces [8].

3. Results and discussion

3.1. Effect of inclusions

Radiographs obtained from unfluxed test bars (50 mm gauge length, 12.5 mm diameter) of the present composite are shown in Fig. 1 for two extreme conditions. Fig. 1a corresponds to filtered test bars, where the inclusions are rated slight (1–2, with reference to ASTM 155), whereas Fig. 1b represents radiographs obtained from unfiltered test bars showing a much higher inclusion density (rated excessive, 7–8).

Recently, Asselin *et al.* [8] proposed a correlation between the maximum inclusion size measured from radiographs and those measured directly from the fractured surfaces of the same test bars, Fig. 2. The marked discrepancy observed in Fig. 2 may be explained in terms of the difficulty in measuring precisely the inclusion size from X-ray radiographs due to lack of contrast. Another factor to be considered is the difference in the plane of measurements in the two cases. The present authors suggest, instead, plotting the volume fraction of inclusions (measured by image analysis of at least 75 fields per sample, performed on polished transverse and longitudinal sample sections immediately beneath the fractured surfaces) against the rating levels of their radiographs. The results are depicted in Fig. 3, where a better relationship is obtained. It should be noted that gas and shrinkage porosity (~ 0.3 vol %) was not considered in Fig. 3. The deleterious effect of inclusions on the tensile properties of the composite, particularly elongation, is displayed in Fig. 4 [9].

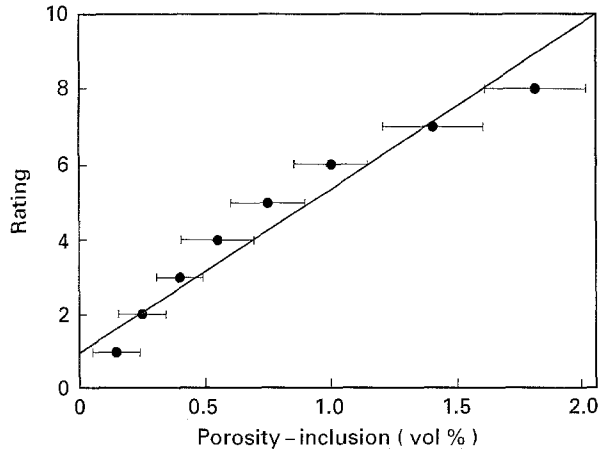

Figure 3 Inclusion volume fraction versus rating relationships.

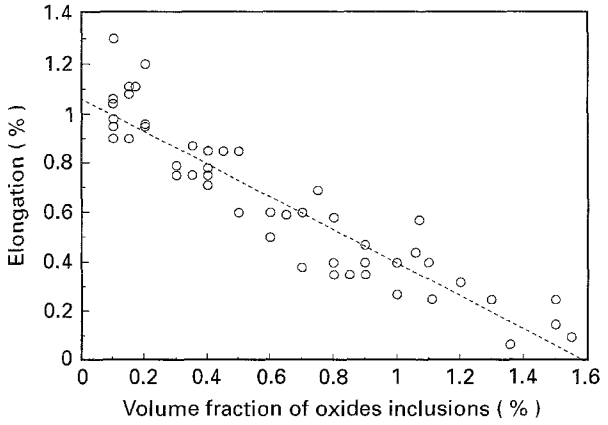

Figure 4 Dependence of elongation on inclusion volume fraction.

3.2. Effect of NaCl contamination

The added dosage of NaCl and the residual content of Na detected by spectral analysis are listed in Table II for the three trial runs that were conducted. It is seen that the residual Na content is no more than 6 p.p.m.

Tensile properties of NaCl contaminated specimens for additions of 10, 40 and 200 p.p.m. NaCl for two different trials are shown in Figs 5 and 6, where each reading represents the average value of the readings obtained from the two test bars produced simultaneously from the same casting. In both cases, it is seen that with the increase in added concentration of NaCl, yield strength (YS) and ultimate tensile strength (UTS) decrease, with the latter exhibiting a slightly stronger decreasing tendency. Correspondingly, the elongation is noted to increase, whereas the Young's modulus remains more or less unchanged or is slightly decreased. These observations may be accounted for by the dewetting of the SiC particles and, hence, their ineffectiveness in reinforcing the matrix. Part of the SiC particles was lost with the floating dross.

A comparison of the microstructures of salt free and NaCl contaminated samples revealed no visible difference. After heat treatment, the eutectic Si particles in the salt free specimens were observed to have an average aspect ratio of 1.43 and an average area of 11.0 μm^2, whereas those in the NaCl contaminated specimens had an average aspect ratio of 1.45 and an average area of 10.5 μm^2.

3.3. Effect of fluxing

The chemical and spectral analysis results of the specimens fluxed with Foseco fluxing agent are shown in Table III. It is seen that compared to NaCl contaminated specimens, fluxed specimens contain higher amounts of residual Na.

Fig. 7a–c displays, respectively, the changes in YS, UTS and per cent elongation as a function of residual (Na + K) content, with reference to the salt free specimen at the starting point. It can be observed that with the increase in (Na + K) residual content, both YS and UTS exhibit a stronger decreasing tendency than that shown by the NaCl contaminated specimens. It is also seen that compared to flux free specimens, fluxed test bars have a higher level of elongation which increases with increasing residual content of (Na + K). These changes are caused by Mg removal in the form of $MgCl_2$ when covering fluxes containing alkali chloride are used to clean the molten metal.

To evaluate the effect of fluxing on changes in the size and shape of the eutectic Si particles, measurements of the area and aspect ratios of the eutectic Si particles were made using image analysis. The correlation of these measurements to the residual (Na + K) content is displayed in Fig. 8. It is seen that the average aspect ratio increases with increasing (Na + K)

TABLE II Residual Na content in NaCl contaminated specimens

NaCl addition (p.p.m.)	Stirring time (min)	Residual Na content (p.p.m.)		
		First trial	Second trial	Third trial
10	20	2	3	4
	40	2	–	–
	60	3	3	3
40	20	2	4	4
	40	2	–	–
	60	3	4	4
200	20	2	5	5
	40	4	–	–
	60	4	6	6

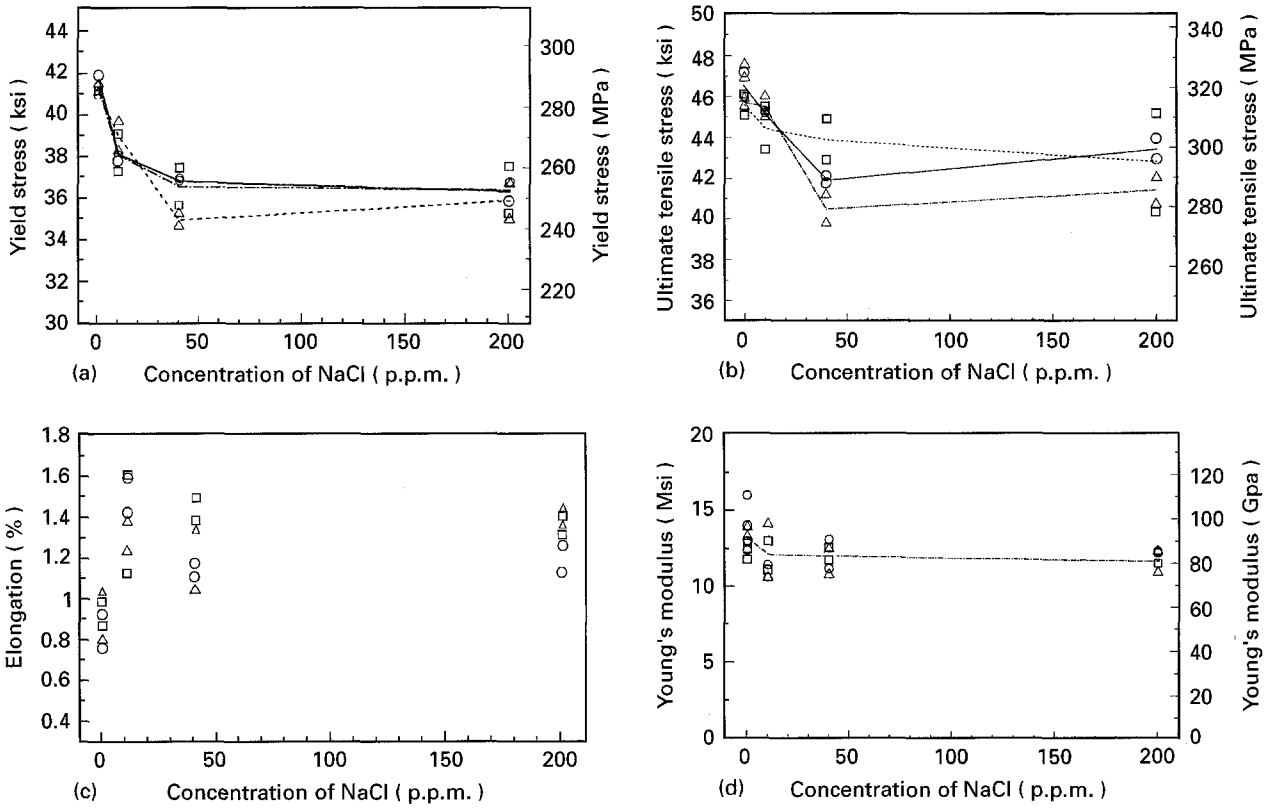

Figure 5 Tensile properties of NaCl contaminated test bars: first trial. (a) yield strength, (b) ultimate tensile strength, (c) per cent elongation, and (d) Young's modulus. (⊖) 20 min stir, (⊟) 40 min stir, (– · △ · –) 60 min stir.

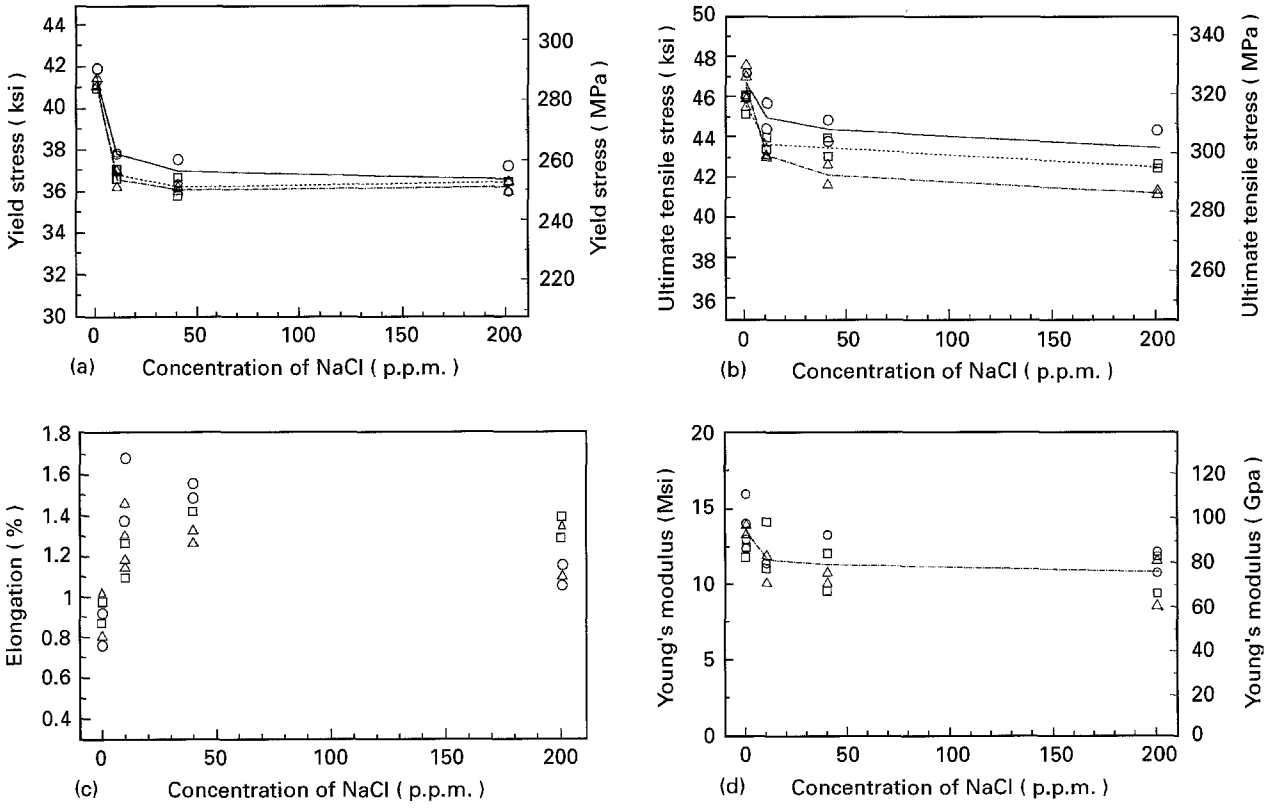

Figure 6 Tensile properties of NaCl contaminated test bars: second trial. (a) yield strength, (b) ultimate tensile strength, (c) per cent elongation, and (d) Young's modulus. (○) 20 min stir, (□) 40 min. stir, (△) 60 min stir.

content, whereas the average area increases, attains a maximum value when (Na + K) is about 60 p.p.m., and thereafter decreases with further increase in (Na + K) content. These findings show that the addition of NaCl negates the modification effect of strontium, resulting in an unmodified structure [10].

An important condition in the use of SiC particles as reinforcement is that the interface bonding between

TABLE III Residual contents of Na and K in fluxed specimens

Stirring time (min)	First trial		Second trial	
	Na (p.p.m.)	K (p.p.m.)	Na (p.p.m.)	K (p.p.m.)
20	8	10	5	10
40	15	17	12	10
60	31	32	66	60

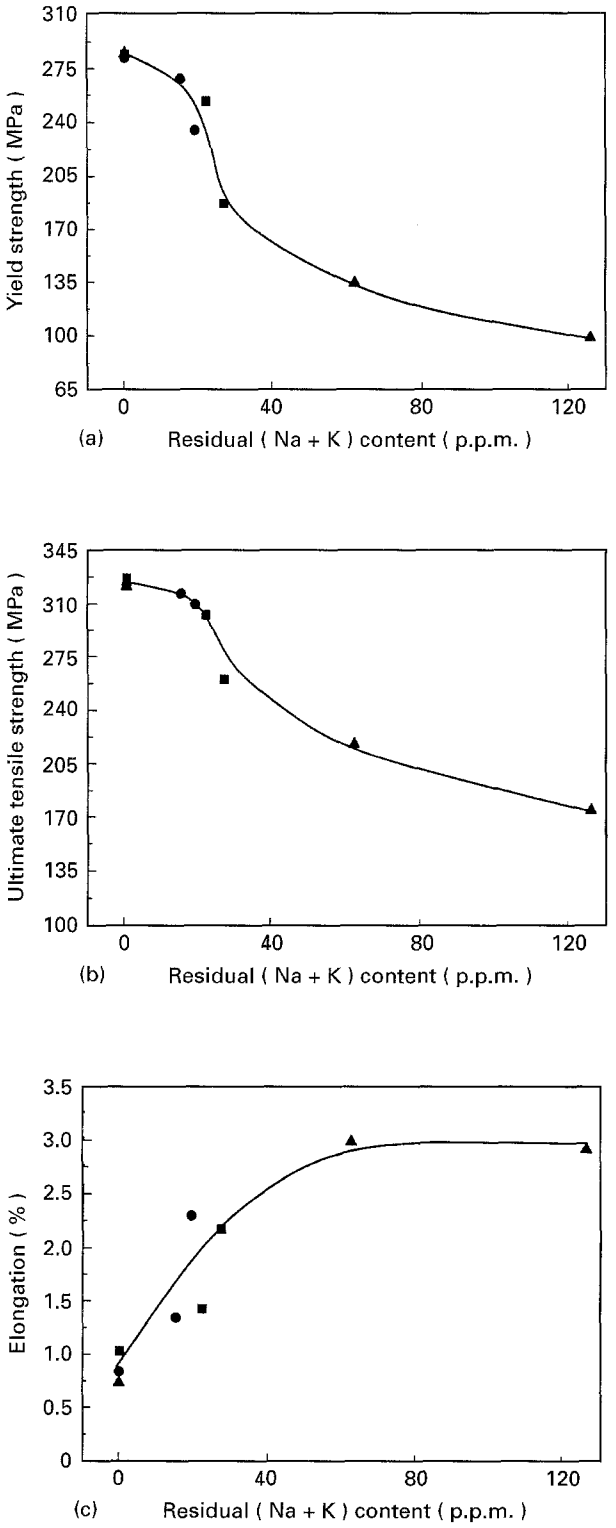

Figure 7 Tensile properties of fluxed test bars (a) yield strength, (b) ultimate tensile strength, and (c) per cent elongation. (●) 20 min stir, (■) 40 min stir, (▲) 60 min stir.

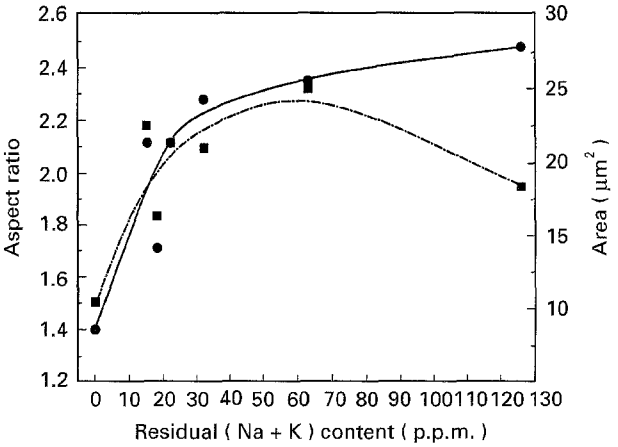

Figure 8 Variation of silicon particle area (■) and aspect ratio (●) as a function of residual (Na + K) content.

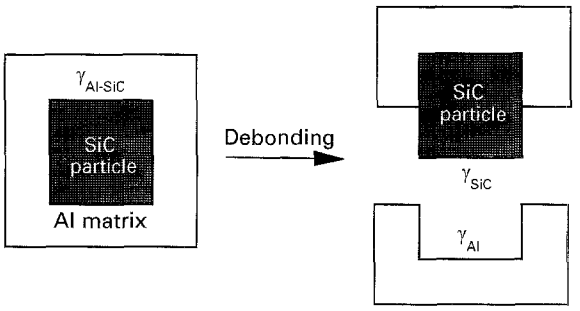

Figure 9 Schematic diagram showing the bonding–debonding process at the molten metal–SiC particle interface.

the SiC particles and the matrix should be adequately strong. The energy dispersive X-ray (EDX) analysis showed the presence of a higher (Na + K) content at the interface than in SiC particle free areas. The presence of Na and K at the SiC_p–matrix interface changes the bonding properties by changing the interface tension. The bonding–debonding process at the interface is schematically depicted in Fig. 9. The bonding strength can be expressed in terms of the work of adhesion, W_{ad} as

$$W_{ad} = \gamma_{Al} + \gamma_{SiC} - \gamma_{Al\text{-}SiC} \quad (5)$$

where γ_{Al} and γ_{SiC} are the surface tensions of the matrix and SiC particle, respectively, and $\gamma_{Al\text{-}SiC}$ is the interface tension between them. For simplicity, only consider the case for Na, for example. According to the Gibbs' adsorption equation, the following relation exists

$$\Gamma = RT[(d\gamma_{Al\text{-}SiC})/(d\ln a_{Na})] \quad (6)$$

where Γ is the excess surface coverage; a_{Na}, the activity of Na in the melt; T, the absolute temperature; and R, the gas constant.

Due to the higher Na concentration at the SiC_p–matrix interface, Γ is known to have a positive value; hence $d\gamma_{Al\text{-}SiC}$ will be negative, resulting in a reduction in the interface tension $\gamma_{Al\text{-}SiC}$. From Equation 6, it is known that a decrease in interface tension, $\gamma_{Al\text{-}SiC}$, will reduce the value of W_{ad} and weaken the interface bonding.

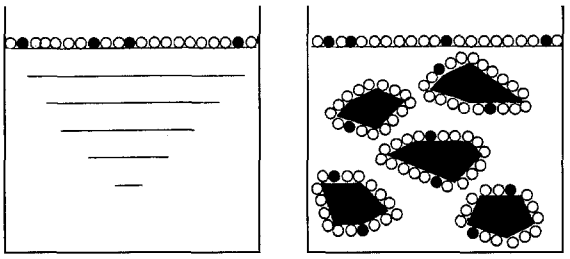

Figure 10 Schematic diagram showing adsorption of Na and K at the SiC particle–Al matrix interface: (a) Al–Si alloy melt, (b) composite melt. (●) Al atom, (○) Na or K atom or flux powders (NaCl, KCl), (◆) SiC particle.

Due to the adsorption of Na and K at the SiC particle–Al matrix interface and that of the fluxing agent powder on the surface of the SiC particles, the influence of the fluxing process is very different in the case of a SiC particle reinforced aluminium composite melt than in the case of an aluminium alloy melt. Fig. 6 schematically depicts the two cases: in the case of a molten Al–Si alloy with an homogeneous melt, there are no surfaces or interfaces in the bulk for Na–NaCl or K–KCl to segregate at or get attached to. Upon solidification, the solute content of these impurities is thus no more than that observed in the liquid state (Fig. 10a). In the case of a SiC_p–Al composite melt, however, the solid SiC particles in the melt provide a large surface for the adsorption of these impurities. After solidification, therefore, all these impurities remain in the solid (Fig. 10b).

4. Conclusions

1. Measuring inclusion size from X-ray radiographs may lead to unreliable results. Instead, inclusion density estimated from X-ray radiographs, i.e. rating, could be used to predict inclusion volume fraction. The latter, in turn, determines the composite mechanical properties.

2. An impurity content of less than 6 p.p.m. Na reduces the YS and UTS while increasing the ductility slightly, but has no noticeable effect on the microstructure of the composite.

3. A mixture of NaCl and KCl in equivalent quantities reduces the YS and UTS, increases the ductility to a certain degree, as well as alters the microstructure and causes dewetting of the SiC reinforcement particle.

4. The effect of a (NaCl + KCl) mixture can be accounted for in terms of the strong tendency of Na and K for adsorption at the SiC particle surface interfaces and the consequent change in surface tension.

5. The eutectic Si particles in the composite alloy matrix become unmodified by the addition of NaCl + KCl thus altering the microstructure.

References

1. J. CAMPBELL, "Castings" (Butterworth Heinemann, Oxford, 1991) pp. 1–26, 268–270.
2. D. M. SCHUSTER, M. D. SKIBO, R. S. BRUSKI, R. PROVENCHER and G. RIVERIN: in SAE International Congress & Exposition, Cobo Centre, Detroit, MI (1993).
3. D. WEBSTER, *Metall. Trans. A* **18** (1987) 281.
4. C. E. RANSLEY and D. E. TALBOT, *J. Inst. Metals* **88** (1959) 150.
5. L. F. MONDOLFO, "Aluminum Alloys: Structure and Properties" (Butterworth, London, 1975) p. 601.
6. R. DEFAY, I. PRIGOGINE, A. BELLEMANS and D. H. EVERETT, "Surface Tension and Adsorption" (Green & Co., London, 1966) p. 158.
7. F. H. SAMUEL, H. LIU and A. M. SAMUEL, *Metall. Trans. A* **24** (1993) 1631.
8. D. ASSELIN, R. PROVENCHER and M. BOUCHARD, in Proceedings of the International Symposium "Development and Applications of Ceramics and New Metal Alloys", Québec City, Québec, 29 August–2 September 1993 edited by R.A.L. Drew and H. Mostaghaci (The Metallurgical Society of the Canadian Institute of Mining, Metallurgy and Petroleum, Montreal, Québec, 1993) pp. 233–243.
9. H. LIU and F. H. SAMUEL, *AFS Trans.* **101** (1993) 739.
10. J. E. GRUZLESKI and B. M. CLOSSET, "The Treatment of Liquid Aluminium–Silicon Alloys" (American Foundrymen's Society, Inc., Des Plaines, IL, 1990) pp. 31–50.

Received 10 April
and accepted 11 May 1995